

Video Article

Multi-photon Imaging of Tumor Cell Invasion in an Orthotopic Mouse Model of Oral Squamous Cell Carcinoma

Amanda Gatesman Ammer¹, Karen E. Hayes¹, Karen H. Martin¹, Lingqing Zhang², George A. Spirou³, Scott A. Weed¹¹Department of Neurobiology and Anatomy, Program in Cancer Cell Biology, Mary Babb Randolph Cancer Center, West Virginia University²Sensory Neuroscience Research Center, West Virginia University³Departments of Otolaryngology and Physiology, Center for Neuroscience, West Virginia UniversityURL: <https://www.jove.com/video/2941>DOI: [doi:10.3791/2941](https://doi.org/10.3791/2941)

Keywords: Medicine, Issue 53, Invasion, mouse model, two-photon microscopy, tongue, orthotopic, head and neck cancer

Date Published: 7/25/2011

Citation: Gatesman Ammer, A., Hayes, K.E., Martin, K.H., Zhang, L., Spirou, G.A., Weed, S.A. Multi-photon Imaging of Tumor Cell Invasion in an Orthotopic Mouse Model of Oral Squamous Cell Carcinoma. *J. Vis. Exp.* (53), e2941, doi:10.3791/2941 (2011).

Abstract

Loco-regional invasion of head and neck cancer is linked to metastatic risk and presents a difficult challenge in designing and implementing patient management strategies. Orthotopic mouse models of oral cancer have been developed to facilitate the study of factors that impact invasion and serve as model system for evaluating anti-tumor therapeutics. In these systems, visualization of disseminated tumor cells within oral cavity tissues has typically been conducted by either conventional histology or with *in vivo* bioluminescent methods. A primary drawback of these techniques is the inherent inability to accurately visualize and quantify early tumor cell invasion arising from the primary site in three dimensions. Here we describe a protocol that combines an established model for squamous cell carcinoma of the tongue (SCOT) with two-photon imaging to allow multi-vectorial visualization of lingual tumor spread. The OSC-19 head and neck tumor cell line was stably engineered to express the F-actin binding peptide LifeAct fused to the mCherry fluorescent protein (LifeAct-mCherry). Fox1^{nu/nu} mice injected with these cells reliably form tumors that allow the tongue to be visualized by *ex-vivo* application of two-photon microscopy. This technique allows for the orthotopic visualization of the tumor mass and locally invading cells in excised tongues without disruption of the regional tumor microenvironment. In addition, this system allows for the quantification of tumor cell invasion by calculating distances that invaded cells move from the primary tumor site. Overall this procedure provides an enhanced model system for analyzing factors that contribute to SCOT invasion and therapeutic treatments tailored to prevent local invasion and distant metastatic spread. This method also has the potential to be ultimately combined with other imaging modalities in an *in vivo* setting.

Video Link

The video component of this article can be found at <https://www.jove.com/video/2941/>

Protocol

1. Cell Lines, Vector Construction and Lentiviral Production

1. Human head and neck tumor cells lines (OSC19 or UMSCC1) were cultured in complete media consisting of DMEM (Cellgro cat # 50-003-PB) supplemented with 10% fetal bovine serum FBS (Hyclone cat # SH30070.03), 1% penicillin/streptomycin (Cellgro cat #30-002-CI), and 1% non-essential amino acids (Cellgro cat # 25-025-CI).
2. To transfer the LifeAct-mCherry coding sequence into the pLL7.0 lentiviral vector, the Sbf1 recognition site in the parent mCherry cDNA was altered by introducing three silent mutations into the recognition sequence using site-directed mutagenesis (Stratagene cat # 200518-5). The resulting modified LifeAct-mCherry sequence was then PCR amplified with flanking EcoR1/Sbf1 sites and subcloned into pLL7.0 to generate the pLL7.0-LifeAct-mCherry construct.

2. pLL7.0-LifeAct-mCherry Virus Production

1. Viral production was conducted according to the Lentiviral Expression Systems manual (System Bioscience version 2-051018).
2. The packaging cell line 293T/17 cells (ATCC cat # CRL-11268) was grown to 40% confluence in the same complete media used for HNSCC lines.
3. Cells were transfected with the pLL7.0-LifeAct-mCherry, psPAX2, and pVSV-G vectors in a 3:2:1 ratio, respectively using CalPhos (Clontech cat # 631312).
4. After 24 hours, the initial media from the transfection was replaced with fresh media.
5. Media was then collected and replenished every 12 hours for 72 hours and stored at 4°C.

3. Production of Head and Neck Cell Lines with Stable LifeAct-mCherry Expression

1. The collected media was spun at 2000 rpm for 10 minutes at 4°C.
2. One ml of clarified media containing virus was directly added to OSC19 or UMSCC1 cells for 12 hours. Cells were then rinsed, and an additional one mL of virus was added for another 12 hour period.
3. Cells were treated with media containing 200mg/ml puromycin for two weeks to select resistant colonies.
4. Surviving clones were screened visually for LifeAct-mCherry expression by fluorescence microscopy. Individual positive colonies were typsinized using sterile 3mm cloning discs (Fisher cat # 0790710A).
5. Positive cells were maintained in media containing 200mg/ml puromycin until frozen back or used for orthotopic injection.

4. Orthotopic Tumor Xenograft Formation

1. All animal procedures were conducted in accordance with a protocol (09-0821) approved by the West Virginia University Animal Care and Use Committee.
2. LifeAct-mCherry expressing tumor cells were trypsinized, centrifuged and 2.5×10^4 cells were resuspended in 50 μ L complete media.
3. Tumor cells were loaded into a one ml syringe attached to a 27 $\frac{1}{2}$ gauge needle.
4. Female athymic Fox1^{nu/nu} mice 8 weeks of age (Harlan Laboratories) were anesthetized with combination of 80mg/kg ketamine and 10mg/kg xylazine. Anesthetized mice were maintained between 37-40 °C on a heating pad.
5. Using sterile forceps, the tip of the tongue was gently grasped and carefully pulled out of the oral cavity.
6. Cells were slowly injected into one side of each tongue to create a bulbous mass in the tongue center, avoiding the lingual arteries.
7. Mice were injected with 2.1mg/kg yohimbine and returned to the heating pad where they were monitored for 2-3 hours during recovery from anesthesia.
8. Once revived, mice were placed into sterile cages containing a soft transgenic dough diet (Bioserve cat # S3472).
9. Mice were weighed every 2-3 days and monitored visually for tumor onset.

5. Preparation of Mouse Tongues for Ex-vivo Imaging

1. Mice harboring tumors at different time points (typically 2-4 weeks post-injection) were euthanized by carbon dioxide inhalation.
2. Tongues were extracted, rinsed with 1X PBS and attached to one side of a conventional paraffin tissue embedding cassette (StatLab Cat #H104,) using monofilament sewing thread from a local hobby shop and a size 8 sewing needle.
3. Once the tongues were immobilized, the entire cassette assembly was placed in a 30mm tissue culture dish and immersed in 1X PBS.
4. Processed tongues were immediately used for two-photon excitation microscopy.

6. Imaging of Tongue Tumors with Two-photon Microscopy

1. Tongue cassettes were submerged in a 60mm dish containing 1X PBS secured in a custom designed holder on a retractable cantilever arm (Chamber Shuttle, Siskiyou instruments) positioned under the objective of an upright microscope (Moveable Microscope (MOM); Sutter Instruments).
2. A 40X/0.8NA water dipping objective lens was placed directly on or over visible tumor lesions. Tongues were imaged by two-photon microscopy with the Ti:sapphire laser (Mira, Coherent) intensity at 60 mW and input wavelength of 755 nm to optimize the mCherry signal.
3. Serial 1mm laser scanning images were collected at 1 μ m incremental depths over a total tissue depth between 15 and 100 μ m (depending on tumor volume). Images were captured using ScanImage, an open source program based on the MATLAB platform that was developed by the Karel Svoboda laboratory (Janelia Farms, HHMI). ScanImage generates a two-channel output of raster scan patterns to control the x/y galvanometric scan mirrors, and at the same time captures a maximum four-channel signal simultaneously from photomultiplier tubes (PMTs) through a data acquisition board (PCI-6610S, National Instruments). The PMT signals are amplified by low noise current preamplifiers (SR570, Stanford Research System) before feeding into the NI-DAQ board for display on the monitor screen. ScanImage collects z-stack images by controlling the z-axis of the objective and collects time-lapse images in a single or cycle mode. Images were saved in a single TIFF file with 16 bit depth.

7. Image Analysis using Amira Software

1. Amira imaging for tumor quantification: In Amira software, open the TIFF file containing the set of z-stack images.
2. Highlight the file name, select and apply the Voltex function to generate a three dimensional rendering. A large primary tumor image with several smaller, dissociated invasive groups (IG) of collectively invaded cells is typically apparent in the rendered image (see Figure 6A).
3. To select the primary tumor mass, select "Open Data", then "Labeling", then "Label Field".
4. Thresholding the primary tumor- select all z-stack images and scroll through the images in the z-plane to ensure inclusion of only the primary tumor mass within three dimensions. This is typically the largest sized image in the field and often appears segmented as the imaged is traversed through the z-plane.
5. Use the magic wand/threshold function to correct background fluorescence and eliminate it from the image without discarding any of the tumor signal. Highlight the "Inside File" label and click the # button. Select the "All Slices" check box. This produces a colored border around the thresholded primary tumor area in every z-stack increment.
6. To select IGs, choose the "New" function. Select a single IG and ensure it is not associated with the primary tumor by scrolling through the z-plane.
7. Select "All Slices" and click the # button. Rename the file (ex: IG 1)
8. Repeat the thresholding procedure in 7.4 and the highlighting step in 7.5 for the determined IG. Select an outline color different than the color used to denote the primary tumor mass.

9. Repeat as necessary for each additional IG throughout the image, scanning through the z-plane to ensure all IGs are denoted. Using different colors for each identified IG aids in future identification on the image.
10. Once the primary tumor and all IGs are selected, select "Segmentation" from the pulldown menu, then select "Material Statistics". This provides the volume measurement as well as the X, Y and X tumor core coordinates for the primary tumor in order to calculate distances of IGs from the central tumor point.
11. With the volumes calculated, determine the distance for each IG from the central core of the primary tumor. Select "Segmentation", then "Material Statistics". This step calculates all measurements into pixels. Convert pixels to micrometers based on the calibration of the microscope objective and any additional increases in magnification (i.e.; zoom functions). For the microscope and settings used in these experiments, the 40X objective was used with no zoom, giving a calibration of 1 pixel = 0.298 μm . Import data into an Excel spreadsheet, which gives parameters for the primary tumor in three dimensions (X1, Y1, Z1) and for each IG (ex: X2, Y2, Z2 for the first IG).
12. The invaded distance in microns for each IG from the center of the primary tumor is calculated using the formula $\sqrt{(X2-X1)^2 + (Y2-Y1)^2 + (Z2-Z1)^2}$.
13. The tumor invasive index (T_i) is calculated using the formula $T_i = N_T \times V_T \times D_T$, where N_T = the total number of IGs in the image, V_T = the total volume of all IGs, D_T = total distance traveled of all invasive groups from the center of the primary tumor.

8. Three dimensional renderings with Nikon NIS-Elements Software

1. Three dimensional renderings with greater topographical detail can be generated by importing the original 16-bit monochrome TIFF files of the entire tumor image into the Nikon NIS-Elements software package (Nikon, Melville, NY). Select "File", then "ND", then "Create ND File from File Sequence". Select the TIFF z-series image stack and specify the appropriate step size.
2. Calibrate the ND document in the xy plane. Specify the size of one pixel using a manual calibration.
3. Choose the "Volume View". Use the "HQ" function to calculate additional slices in the z-plane for higher quality. In the "3D Renderer Settings", use the "Advanced Renderer" with a quality of "Ultra High Details" and "Full Resolution". Choose "Alpha Blending" to accentuate the tumor surfaces.
4. Optimize the three-dimensional image for presentation. Zoom in on the tumor and associated IGs and crop as needed. Rotate the image in the xyz planes and adjust the LUTs.
5. Capture the image for presentation. Select "Edit- Create View Snapshot (8 bit RGB)". Name and save file accordingly.

9. Representative Results

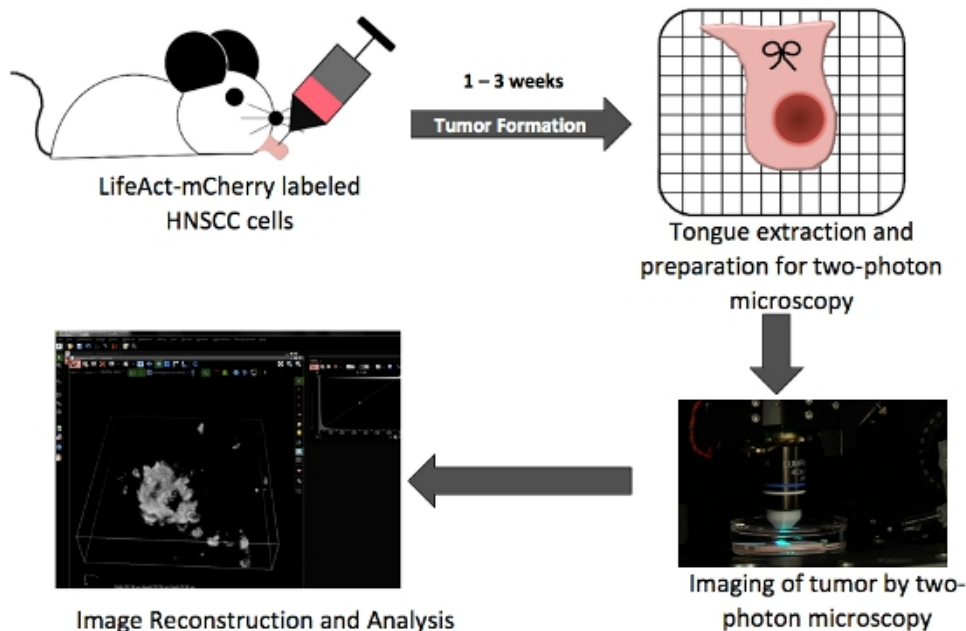


Figure 1. Overall schematic illustrating key steps in orthotopic tongue tumor production and in situ two photon imaging.



Figure 2. Injection of LifeAct-mCherry expressing OSC19 cells into the mouse tongue.

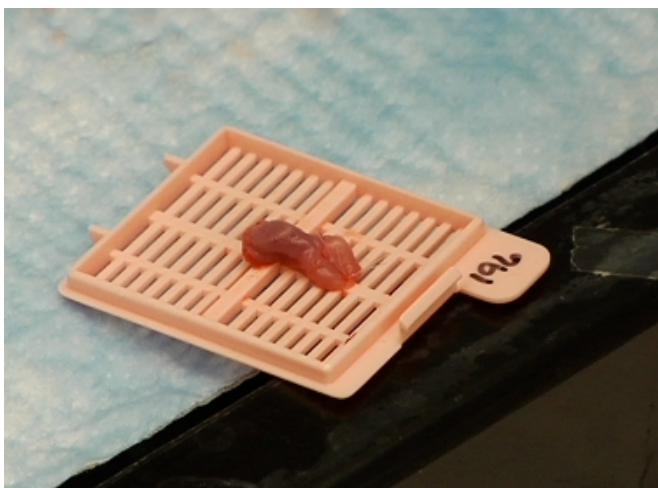


Figure 3 Resected tumor-containing mouse tongue prepared for two photon imaging.

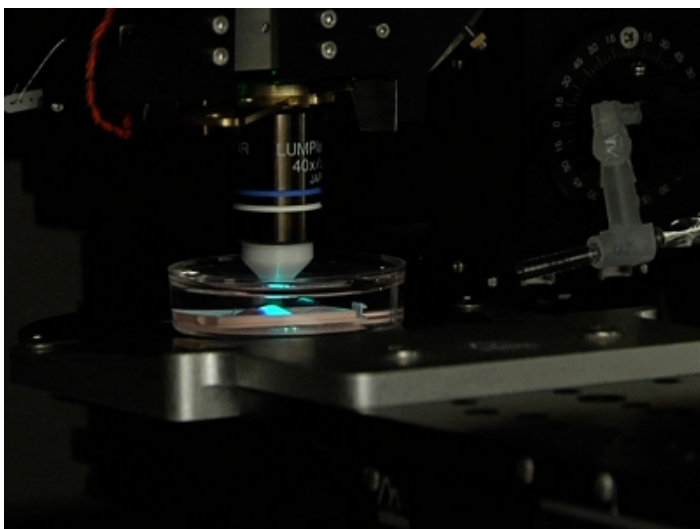


Figure 4. Orientation of a tumor-containing tongue in position on a two photon microscopy ready for imaging.

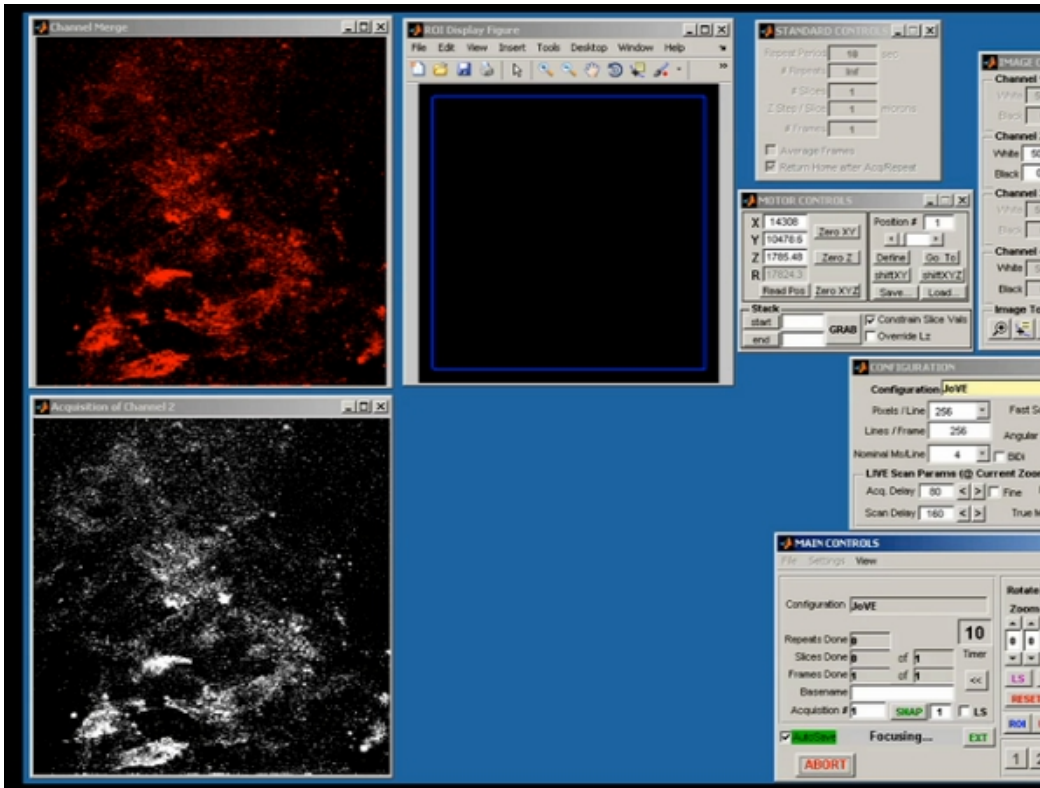


Figure 5. Representative screen shot from ScanImage demonstrating raw data acquisition of the initial two-photon image.

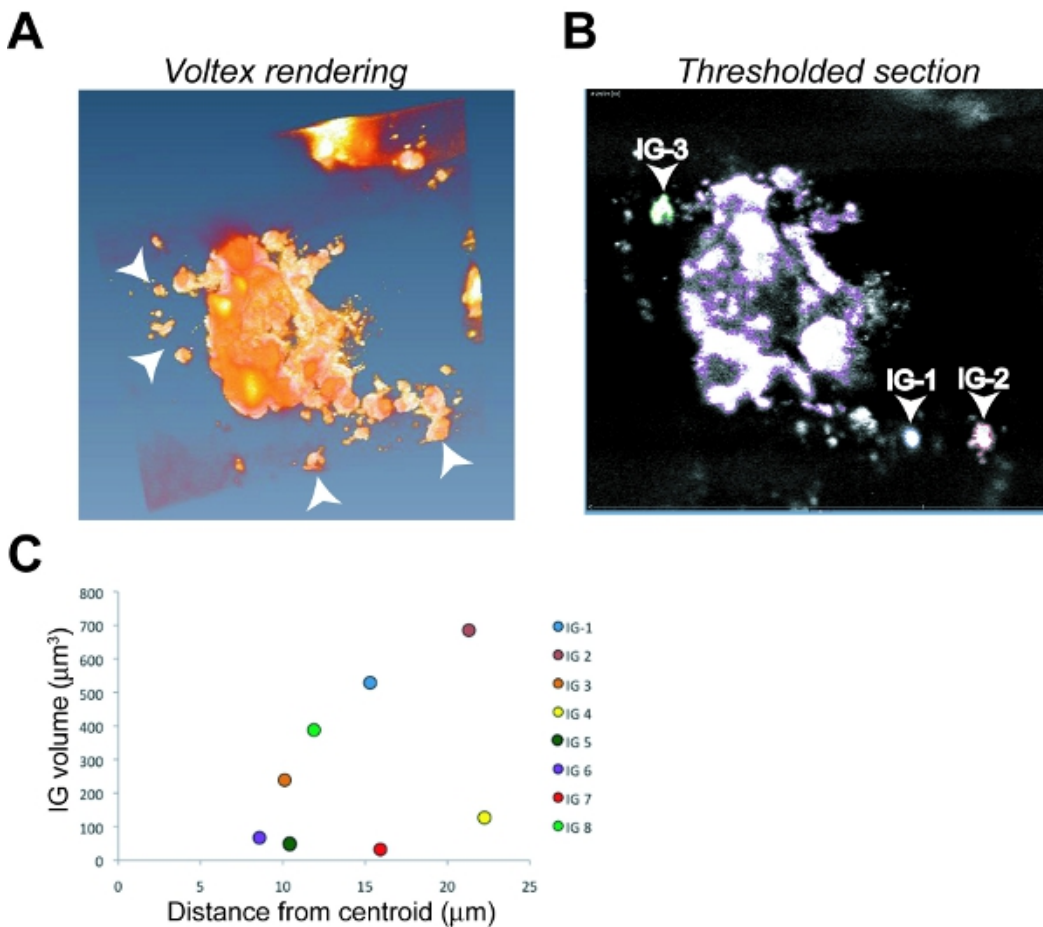


Figure 6. Image analysis and quantification of tumor invasion in an orthotopic OSC19 tumor. Representative screen shot images of Amira Voltex rendering (A) and a single thresholded z-section (B) with the primary primary tumor outlined in purple, invasive group 1 (IG-1) outlined in blue, IG-2 outlined in red and IG-3 outlined in green as an example of the identification procedure. Arrowheads denote IGs in (A) and (B). C. Plots of volume versus invaded distance for eight individual IGs used to calculate the tumor invasion index (Ti).

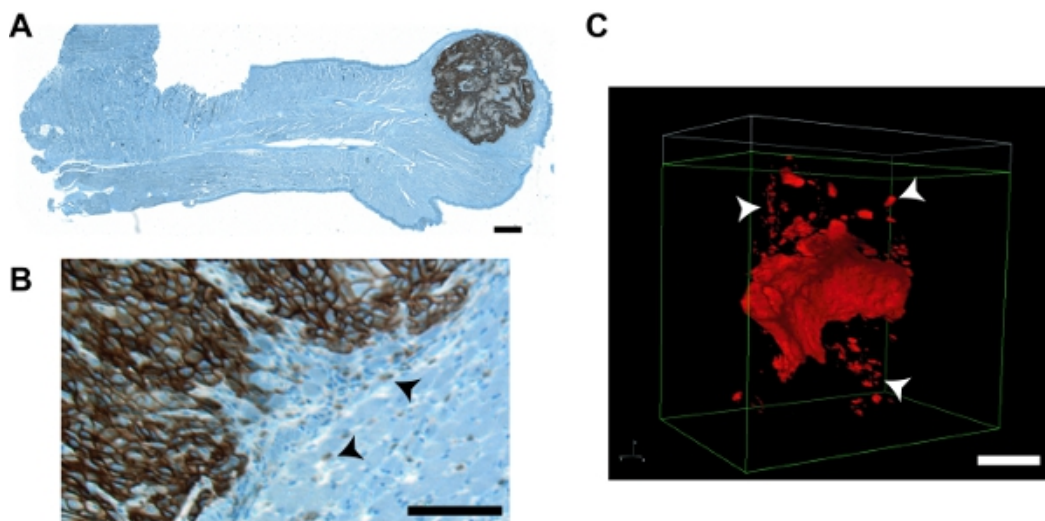


Figure 7. Representative images of tumors and invaded tumor groups from this protocol compared with images from a conventional IHC approach. A. Paraffin section of an entire mouse tongue harboring a UMSSC1 orthotopic tumor. Immunohistochemical staining was conducted using conventional procedures with a primary antibody against the HNSCC-specific cell marker emmprin (Zymed; cat # 34-5600) at 1:1000 dilution and visualized by using the OmniMap DAB anti-Rb detection kit (Ventana cat # 760-149) followed by iron hematoxylin staining. Images encompassing the total tongue area were collected individually at 4X magnification on an Olympus ZX70 Provis microscope with an Optronics MicroFire CCD camera and reconstructed using the StereoInvestigator imaging package (MBF Bioscience). The tumor is evident at the tongue tip. An enlarged region showing the invasive front and individual tumor cell groups (arrowheads) is shown in (B). C. Nikon NIS-Elements rendering of a representative OSC19 tumor. Enhanced contour detail and clear visualization of IGs (arrowheads) is evident. Bars in all images = 100 μ m.

Discussion

Orthotopic mouse models have proven useful for studying many aspects of head and neck cancer^{1,2}. We have combined a well established orthotopic system of SCOT³ with two-photon microscopy imaging of mCherry-labeled cells as a system to study the early events of head and neck tumor cell invasion. In this procedure, we have noted that cells can leak from the site of tumor injection, especially in mice six weeks or younger due to insufficient tongue size. We use older mice to avoid this issue. The larger tongue size with older mice also aids in avoiding rupture of a lingual artery and excessive hemorrhaging from the tongue. Tumor take is greatly enhanced when the tongue dramatically swells at the site of initial injection. This swelling subsides within one-two hours as the injected fluid is absorbed. Tumor growth appears evident one-two weeks post injection with the indicated injected cell number as a small white bump on the tongue surface. We also note that at the 40X objective used in our studies presented here, we cannot distinguish individual tumor cells but do identify IGs as invasive cell clusters that recapitulate the typical mode of HNSCC invasion.

To date this model has been extensively used for testing the role of specific molecules as well as several anti-tumor drugs on SCOT growth an invasion, with efficacy measured by cervical lymph node metastasis monitored using IHC or bioluminescent methods^{4,7}. Tumors formed in this system manifest close to the tongue surface (Figure 7), allowing the application of two-photon microscopy to image entire tumors in situ as invasive multi-cellular clusters. The procedure can also be utilized to visualize tumor invasion with cellular resolution. Two-photon microscopy has been previously utilized to study experimental treatments for head and neck cancer in orthotopic^{8,9} and xenograft^{8,10} models. However, there are two major differences between these reports and our protocol. First, these studies use extracellular labels to target/identify head and neck tumor cells, possibly limiting detection only to tumor cells with ample access to the circulation. Second, invasion of tumor cells close to the primary site that likely recapitulates early metastatic activity was not assessed as an experimental parameter. Our protocol provides the ability to directly quantify tumor cell invasion at any point during tumor progression in mouse tongues. While the method described here describes the procedure using dissected tongues, we are currently in the process of adapting this method to image tumor invasion in live mice for use in combination with bioluminescence to simultaneously monitor early invasion, local lymph node involvement and distant metastasis in the same animal. Alterations to the protocol for in vivo imaging require designing of an appropriate stage for positioning and maintaining mice during imaging, as well as a practical system to properly irrigate the oral cavity of anesthetized mice during the imaging procedure. Once optimized, these adaptations will provide the ability to study the role of potential pro-invasive molecules and the testing anti-invasive compounds on local invasion and more distant metastatic involvement in animals over extended time periods.

Disclosures

The authors have nothing to disclose.

Acknowledgements

Supported by a subproject of NIH grant P20 RR16440 and a bridge grant from the West Virginia University Office of Research and Graduate Education to S. Weed. Technical assistance from L. Lopez-Skinner during the early phases of project development is gratefully acknowledged. The authors are also grateful for technical assistance and OSC19 cells from J. Myers and M. Younes (Department of Head and Neck Surgery, M.D. Anderson Cancer Center, Houston, TX); P. Turner and K. Secrest (West Virginia University Department of Pathology Tissue Bank) for histological processing and procedures, R. Wysolmerski (West Virginia University, Department of Neurobiology and Anatomy) for the LifeAct-mCherry construct and J. Bear (University of North Carolina) for the pLL7.0 lentiviral vector. The use of the West Virginia University Microscopy Imaging Facility (supported by NIH grant P20 RR16440 and the Mary Babb Randolph Cancer Center) and its non-linear optical microscopy laboratory (NLOM; supported by a joint collaboration between the West Virginia University Center for Neuroscience and the West Virginia University Department of Physics/West Virginia Nanoscience Initiative) is also gratefully acknowledged. The NLOM is supported in part by NIH grant P30 RR031155 to the Center for Neuroscience.

References

1. Sano, D., & Myers, J. N. Xenograft models of head and neck cancers. *Head Neck Oncol.* **1**, 32, doi:1758-3284-1-32 [pii] 10.1186/1758-3284-1-32 (2009).
2. Kim, S. Animal models of cancer in the head and neck region. *Clin Exp Otorhinolaryngol.* **2**, 55-60, doi:10.3342/ceo.2009.2.2.55 (2009).
3. Myers, J. N., Holsinger, F. C., Jasser, S. A., Bekele, B. N., & Fidler, I. J. An orthotopic nude mouse model of oral tongue squamous cell carcinoma. *Clin Cancer Res.* **8**, 293-298 (2002).
4. Sano, D., & Myers, J. N. Metastasis of squamous cell carcinoma of the oral tongue. *Cancer Metastasis Rev.* **26**, 645-662 (2007).
5. Sano, D. *et al.* The effect of combination anti-endothelial growth factor receptor and anti-vascular endothelial growth factor receptor 2 targeted therapy on lymph node metastasis: a study in an orthotopic nude mouse model of squamous cell carcinoma of the oral tongue. *Arch Otolaryngol Head Neck Surg.* **135**, 411-420, doi:135/4/411 [pii]10.1001/archoto.2009.14 (2009).
6. Kupferman, M. E. *et al.* TrkB induces EMT and has a key role in invasion of head and neck squamous cell carcinoma. *Oncogene.* **29**, 2047-2059, doi:onc2009486 [pii]10.1038/onc.2009.486 (2010).
7. Ammer, A. G. *et al.* Saracatinib Impairs Head and Neck Squamous Cell Carcinoma Invasion by Disrupting Invadopodia Function. *J Cancer Sci Ther.* **1**, 52-61, doi:10.4172/1948-5956.1000009 (2009).
8. Rosenthal, E. L., Kulbersh, B. D., King, T., Chaudhuri, T. R., & Zinn, K. R. Use of fluorescent labeled anti-epidermal growth factor receptor antibody to image head and neck squamous cell carcinoma xenografts. *Mol Cancer Ther.* **6**, 1230-1238, doi:6/4/1230 [pii]10.1158/1535-7163.MCT-06-0741 (2007).
9. Gleysteen, J. P. *et al.* Fluorescent labeled anti-EGFR antibody for identification of regional and distant metastasis in a preclinical xenograft model. *Head Neck.* **30**, 782-789, doi:10.1002/hed.20782 (2008).
10. Bhirde, A. A. *et al.* Targeted killing of cancer cells in vivo and in vitro with EGF-directed carbon nanotube-based drug delivery. *ACS Nano* **3**, 307-316, doi:10.1021/nn800551s (2009).